Structure and tribological properties of MoS_2 low friction thin films

Agnieszka Paradecka[1,*], *Krzysztof* Lukaszkowicz[1], *Jozef* Sondor[2], and *Mieczysław* Pancielejko[3]

[1]Silesian University of Technology, Institute of Engineering Materials and Biomaterials, 44-100 Gliwice, Poland
[2]LISS, a.s., Dopravni 2603, 756 61 Roznov p.R., Czech Republic
[3]Koszalin University of Technology, Department of Technical Physics and Nanotechnology, 75-453 Koszalin, Poland

Abstract. The main aim of the studies was the deposition of the AlCrN film, covered by molybdenum disulphide (MoS2) – based lubricant, on the austenitic steel substrate. The AlCrN and MoS2 layers were deposited by PVD lateral rotating ARC-cathodes (LARC) and magnetron sputtering technology on the X6CrNiMoTi17-12-2 respectively. Structural characterizations of the MoS_2 thin films have been carried out using SEM (scanning electron microscopy) and AFM (atomic force microscopy) to determine the surface topography as well as HRTEM (high-resolution transmission electron microscopy) and Raman spectroscopy for structural investigations. The tribological wear relationships using ball-on-disc test were specified for surface layers, determining the friction co-efficient and mass loss of the investigated surfaces. Tests of the coatings' adhesion to the substrate material were made using the scratch test. HRTEM investigation shows an amorphous character of the MoS_2 layer. In sliding dry friction conditions, the friction co-efficient for the investigated elements is set in the range between 0.4-0.5. The investigated coating reveals high wear resistance. The coating demonstrated a dense cross-sectional morphology as well as good adhesion to the substrate. The good properties of the PVD AlCrN+MoS_2 coatings make them suitable in various engineering and industrial applications.

1. Introduction

The modern way of countering the harmful effects of friction for the elements of machines working under fixed tribological load is the use of solid lubricants in the form of thin films or coatings on sliding surfaces. These films provide protection in trying conditions, chemical stability, low coefficient of friction and abrasion resistance [1, 2].

One of the most interesting low-friction coatings is molybdenum disulphide (MoS_2), mainly used as a friction reducer in dry, vacuum and inert gases [3, 4]. The fundamental problem in the use of MoS_2 as a solid lubricant is a deterioration of its tribological properties in a humid environment. The reaction of MoS_2 and H_2O formed MoO_3 and H_2S (gaseous). MoO_3 shows a higher shear strength, which contributes to increased coefficient friction and the reduced lifetime of coated components. However, the sensitivity to the humidity of pure MoS_2 coatings can be reduced by, e.g. adding Ti, Cr, C, Al, Au and TiN, or increasing their density [5, 6]. Currently, MoS_2 coatings with the addition of Ti can be used not only in a vacuum or zero relative humidity but also at up to 50% humidity without losing their tribological properties, which allowed the extensive use of terrestrial applications [6].

In the category solid lubricant coatings MoS_2 is classified as soft. The anisotropic crystal structure is influenced by the good tribological properties [7]. These coatings can be applied to the steel substrate by bonding, burnishing, and more modern methods such as physical vapour deposition, which allow better adhesion to the substrate and amorphous structure of the coatings [3, 4, and 7]. The MoS_2 coating lubrication system is derived from a honeycomb structure that consists of a hexagonal array where the molybdenum atoms are surrounded by six sulphur atoms placed at corners of a triangular prism. Strong covalent bonds occur between atoms in layers (atom S and atom Mo_2), and weaker van der Waals forces between adjacent layers (S-Mo-S) allow for a low friction coefficient. The triple layer (S-Mo-S) can exist in three variants: the hexagonal (2H-MoS_2), the rhombohedral (3R-MoS_2) and the trigonal (1T-MoS_2) of which only hexagonal exhibit a low coefficient of friction [8]. In addition, the lubrication effect is extended by transferring the MoS_2 molecules to ablated areas [9]. Particularly important here is film-substrate adhesion, where the stronger it is, the longer the shelf life of the film [6]. MoS_2 coatings are widely used in space applications and industry (e.g. bearings, blades and vanes of turbine engines, HCCI engines, aircraft engines). The development of nanomaterials has allowed them to use their physical properties in nanocomposites,

* Corresponding author: agnieszka.paradecka@polsl.pl

for next-generation electronic devices and nano-electro-mechanical systems and optoelectronics [5, 8, 10-13].

The aim of this paper was to examine the microstructure, and tribological properties of MoS_2 films with additional hard AlCrN interlayer deposited on the austenitic steel X6CrNiMoTi17-12-2.

2. Experimental details

The examinations were made on the X6CrNiMoTi17-12-2 austenitic steel (substrates are cylindrical with 30 mm base diameter and 5 mm thickness) disk covered by AlCrN+MoS_2 coating.

The AlCrN film was deposited in the unit π1511 based on PLATIT's rotating and planar ARC-technology. The coatings deposition was carried out in an Ar and N_2 atmosphere. Cathodes containing pure metal Cr and Al were used for coatings deposition. After pumping the chamber to a base pressure below 5×10^{-5} Pa the substrate was heated to an appropriate temperature. Then, the substrates were cleaned by argon ion at a pressure of 2 Pa and applied bias voltage of 600 V/400 V for 20 min. To improve the adhesion of the coatings, after heating and both cleaning steps the LARC cathode (Cr) was burnt and formed of CrN adhesion layer. The MoS_2 topcoat was deposited by the magnetron sputtering method in the unit PLATIT Pl200. The deposition conditions are summarized in Table 1.

Table 1. Coating deposition parameters.

Parameter	AlCrN	MoS_2
Working pressure [Pa]	3	-
Substrate bias voltage [V]	60	-
Arc of target/magnetron [A]	250/235	1.2
Process temperature [ºC]	450	80
Time [s]	4200	1640

The cross section of the deposited coatings was mapped with the use of the SUPRA 35 scanning electron microscope (SEM). The detection of secondary electrons was used for generation of fracture images with 4 kV bias voltage.

Diffraction and thin film microstructure was tested with the use of the TITAN 80-300 ultrahigh resolution scanning/transmission electron microscope. The thin cross-section lamellas for Transmission Electron Microscopy (TEM) observations were prepared by Focused Ion Beam (FIB) technique using Quanta 200i instrument with gallium ions.

Raman measurements were performed at room temperature with an in Via-Raman microscope (Renishaw) with a 633 nm Ar^+ laser, with a resolution 1 cm^{-1}.

The topography of the samples was examined using the atomic force microscope (AFM) Park System X E-100.

Adhesion of the coating to the substrate material was verified by the scratch test on the CSEM REVETEST device, by moving the diamond indenter along the examined specimen's surface with gradually increasing the load. The tests were made using the following parameters: load range: 0–100 N, load increase rate (dL/dt): 100 N/min, indenter's sliding speed (dx/dt): 10 mm/min.

The friction coefficient and wear rate of the coating were determined in the ball-on-disc test. The tests were carried out on the THT (CSM Instruments) device with the following parameters: sliding speed: 0.2 m/s; normal load: 10 N; counterpart: Al_2O_3 of 6 mm diameter; sliding distance: 1000 m; temperature: 23ºC (±1ºC); relative humidity: 26% (±3%).

3. Results and discussion

The cross-section of the investigated coating is presented in Fig. 1. The coating presents a compact structure; there is no trace of any coating delamination. The morphology of the MoS_2 layer is characterized by a porous microstructure. The clear boundary line is visible between AlCrN and MoS_2 layers. The adhesion layer between AlCrN and steel substrate is not as well defined but still visible on the SEM image. The measured thickness values of the particular layers MoS_2, AlCrN and adhesion layers (CrN) are approximately 1.2 μm, 2.0 μm and about 130 nm, respectively.

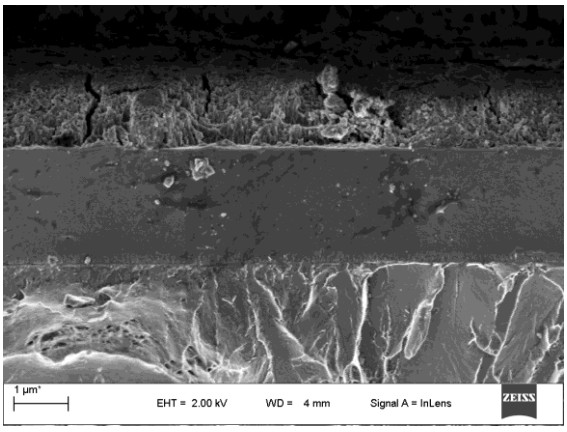

Fig. 1. The cross-section image (SEM) of AlCrN+MoS_2 coating deposited on the steel substrate.

Subsequently, for the coating structure characterization, TEM and HRTEM microscopes were used. The images, presented in Fig. 2, were obtained from selected regions. The bright-field images (Fig. 2a) and the HRTEM micrograph (Fig. 2b) show an amorphous character of the MoS_2 films. As expected, the electron-diffraction patterns obtained show a considerable broadening of diffraction rings (the inset image in Fig. 2a).

In the case of the AlCrN layer, it can be concluded, based on HRTEM images, that the investigated layer has a nanocrystalline structure (Fig. 3). It was found, by examining thin lamellas from the cross section of AlCrN layer produced by the arc method, that the layer features a compact structure with high homogeneity and grain size is less than 10 nm.

The observations of the analysed coatings surface topography using the AFM revealed that the AlCrN/MoS_2 is characterised by a high inhomogeneity relating to multiple droplet-shaped or nearly ball-shaped particles existing on the surface (Fig. 4).

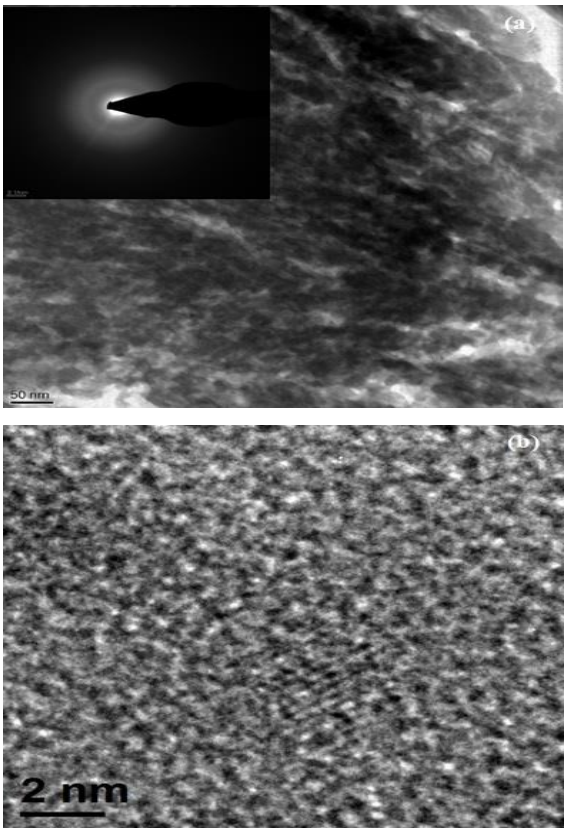

Fig. 2. MoS_2 top layer: a) TEM bright-field image and electron diffraction pattern, b) HRTEM micrograph.

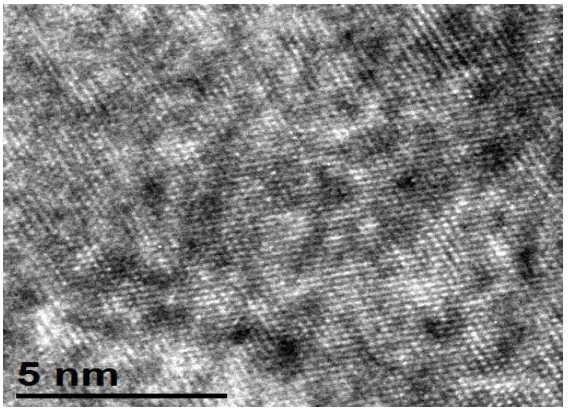

Fig. 3. HRTEM micrograph of the AlCrN layer.

An additional surface development analysis performed determining a ratio of the actual area measured for a given specimen according to its orthogonal projection on the XY plane revealed a large development for hard nitride layers. Surface development increases by about 10 % according to the coating type as a consequence of depositing a low-friction layer onto the surface of nitride layers. The measurements taken also allowed us to determine the layers surface roughness (by R_a).

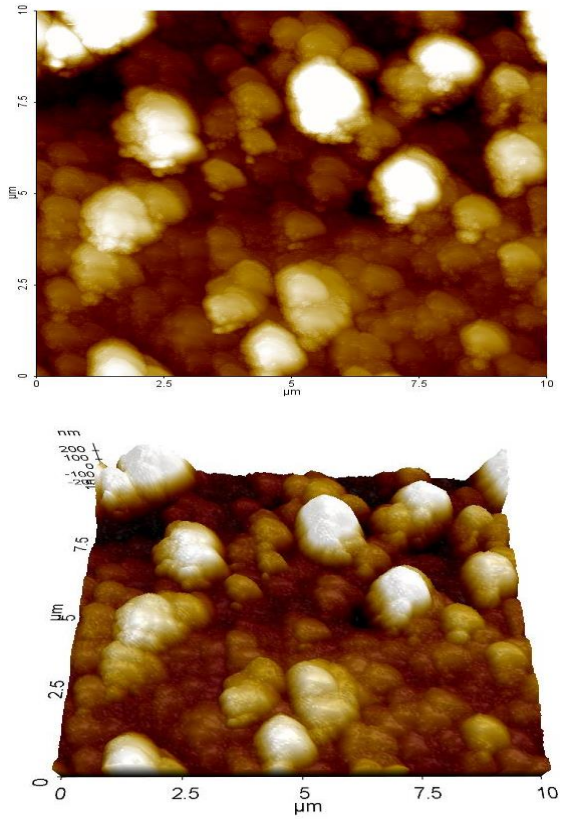

Fig. 4. Two- and three-dimensional AFM images of AlCrN+MoS_2 thin films

Raman spectroscopy shows first-order bands a result of vibrational modes within the S–Mo–S layer (227 cm^{-1}, 313 cm^{-1}, 354 cm^{-1}, 453 cm^{-1}) (Fig. 5). Additional recorded peaks 489 cm^{-1} and 566 cm^{-1} belong to the second-order lines derived from resonance type of Raman Effect. The noticed peaks 202 cm^{-1} and 726 cm^{-1} come from MoO_2 bonds. Visible broadening further on in the spectrum is due to the amorphous structure of layer [14, 15].

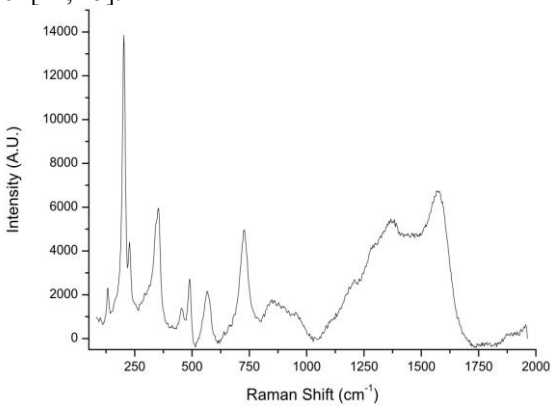

Fig. 5. Raman spectra of AlCrN+MoS_2 coating.

Critical load values L_{C1} and L_{C2} were determined using the scratch-test method with a linearly increasing load, characterizing the adhesion of the investigated coatings to the steel substrate (Fig. 6). The load at which the first coating defects appear is known as the first critical load, L_{C1}. The first critical load, L_{C1}, corresponds to the point, at which the first damage is observed (Fig. 7a); the first appearance of micro-cracking, surface flaking outside or inside the track without any exposure of the substrate material – the first cohesion – indicates a failure event. The second critical load, L_{C2}, is the point at which a complete delamination of the coating starts; the first appearance of cracking, chipping, spallation and delamination outside or inside the track with an exposure of the substrate material – the first adhesion – indicates a failure event (Fig. 7b). The investigated coating shows relatively good values of the critical load. The first failure occurs at a value of ~14 N. The second critical load, L_{C2}, occurs at 48 N. This may be caused by a significantly lower hardness of the X6CrNiMoTi17-12-2 steel substrate (in compare of tool steel).

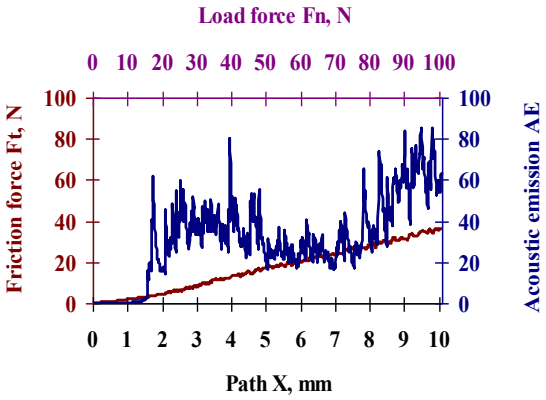

Fig. 6. Acoustic emission (AE) and friction force F_t as a function of the load Fn for AlCrN+MoS_2 coating.

To determine the tribological properties of the AlCrN+MoS_2 coating, an abrasion test under dry slide friction conditions was carried out by the ball-on-disk method. Fig. 8 presents the graph of friction coefficient μ changes obtained during wear tests in relation to counterpart with Al_2O_3. The friction curve has an initial transitional state of an un-stabilized course, during which the friction coefficient is reduced along with the growth of sliding distance up to obtaining the stabilized state, which normally occurs after a distance of about 100 m.

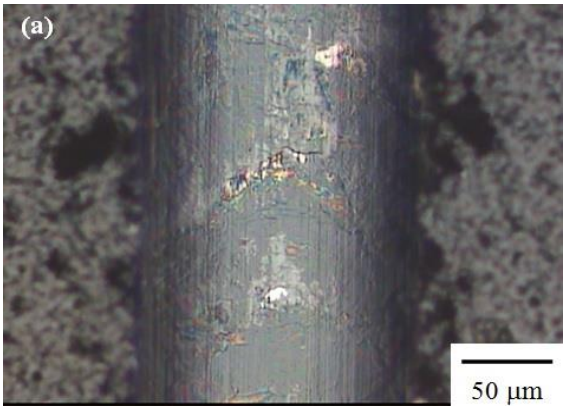

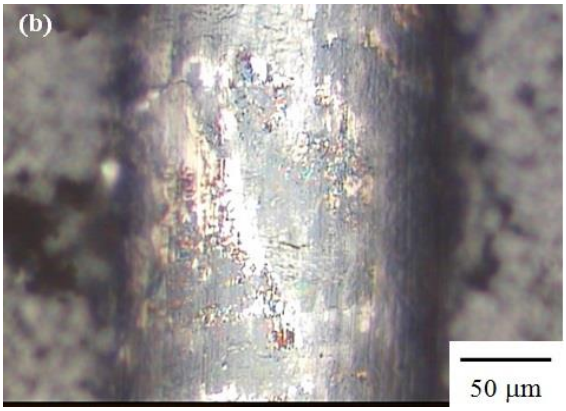

Fig. 7. Scratch-failure images of the AlCrN+MoS_2 coating at: a) L_{C1}, b) L_{C2}.

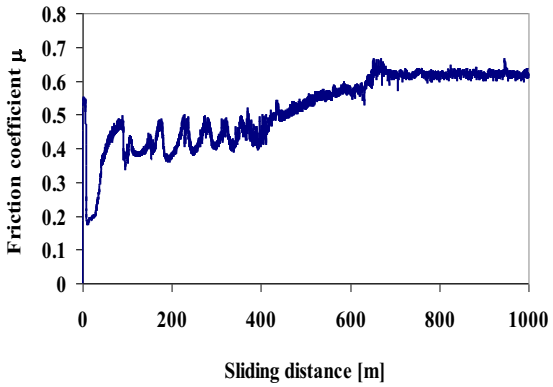

Fig. 8. Dependence of the friction coefficient on the sliding distance during the wear test for the AlCrN+MoS_2 coating.

Under technically dry friction conditions, after the wearing-in period, the friction coefficient recorded for the associations tested is stabilized in the range 0.4–0.5. There was no case of the coatings wearing through completely because the maximum wear-in depths were below their thicknesses.

4. Conclusion

The AlCrN+MoS_2 coating was deposited successfully on the X6CrNiMoTi17-12-2 steel substrate. The dense microstructure of the coating without any visible delamination was observed in the scanning electron microscope. Tests using the TEM confirmed an amorphous character of a low-friction MoS_2 layer. Under the technically dry friction conditions, the friction coefficient for the associations tested is within the range 0.4-0.5 for the investigated coating. The scratch tests on coating adhesion reveal the cohesive and adhesive properties of the coatings deposited on the substrate material.

References

1. T. Hu, Y. Zhang, L. Hu, Wear **278-279** (2012)
2. K. Lukaszkowicz, J. Sondor, K. Balin, J. Kubacki, Appl. Surf. Sci. **312** (2014)

3. T. Kubart, T. Polcar, L. Kopecky, R. Novak, D. Novakova, Surf. Coat. Tech. **193** (2005)
4. L. Rapoport, A. Moshkovich, V. Perfilyev, I. Lapsker, G. Halperin, Y. Itovich, I. Etsion, Surf. Coat. Tech. **202** (2008)
5. B. Vierneusel, T. Schneider, S. Tremmel, S. Wartzack, T. Gradt, Surf. Coat. Tech. **235** (2013)
6. N.M. Renevier, J. Hamphire, V.C. Fox, J. Witts, D.G. Teer, Surf. Coat. Tech. **142-144** (2001)
7. S. Sivarajan, R.P. Padmanabhan, Mater. Today-Proc. **3** (2016)
8. A. Abinaya, B.G. Jeyaprakash, Mat. Sci. Semicon, Proc. **31** (2015)
9. B. Behrens, H.J. Maier, S. Hubner, C.Bonk, A. Almohallami, C. Lummer, P. Scheint, H. Scheland, M. Micke-Camuz, Procedia Eng. **183** (2017)
10. C. Wang, H. Li, Y. Zhang, Q. Sun, Y. Jia, Tribol. Int. **77** (2014)
11. G. Colas, A. Saulot, E. Regis, Y. Berthier, Wear **330-331** (2015)
12. R.B. Pujari, A.C. Lokhande, A.R. Shelke, J.H. Kim, C.D. Lokhande, J. Colloid Interf. Sci. **496** (2017)
13. J. Theerthagiri, R.A. Senthil, B. Senthilkumar, A. Polu, J. Madhavan, M. Ashokkumar, J. Solid State Chem. **252** (2017)
14. B. C. Windom,W. G. Sawyer, D W. Hahn, Tribol. Lett. **42** (2011)
15. M. Dieterle, G. Mestl, Chem. Phys. **4** (2002)